Molecular Structures and Magnetochemistry of Two (β-Oxooctaethylchlorinato)copper(II) Derivatives: [Cu(oxoOEC)] and [Cu(oxoOEC•)]$SbCl_6$

Teresa J. Neal,[†] Seong-Joo Kang,[†,§] Charles E. Schulz,*[,‡] and W. Robert Scheidt*[,†]

The Department of Chemistry and Biochemistry, University of Notre Dame, Notre Dame, Indiana 46556, and The Department of Physics, Knox College, Galesburg, Illinois 61401

Received March 16, 1999

The preparation and characterization of the β-oxochlorin derivative [3,3,7,8,12,13,17,18-octaethyl-(3*H*)-porphin-2-onato(2−)]copper(II), [Cu(oxoOEC)], and its π-cation radical derivative, [Cu(oxoOEC•)][$SbCl_6$], are described. Both compounds have been characterized by single-crystal X-ray structure determinations; IR, UV/vis/near-IR, and EPR spectroscopies; and temperature-dependent magnetic susceptibility measurements. Crystals of [Cu(oxoOEC)] have two crystallographically distinct molecules, one at a general position ([Cu(oxoOEC)]-gen) and a second at a special position ([Cu(oxoOEC)]-spe). [Cu(oxoOEC)]-gen has a S_4-saddled conformation whereas [Cu(oxoOEC)]-spe has a modest ruffled conformation. [Cu(oxoOEC•)][$SbCl_6$] shows a cofacial dimeric unit in the solid state, with a mean plane separation of 3.41 Å and a lateral shift of 5.47 Å. Crystal data for [Cu(oxoOEC)]: monoclinic, space group $C2/c$, $Z = 12$, $a = 38.404(8)$ Å, $b = 14.692(6)$ Å, $c = 16.977(11)$ Å, $\beta = 101.46(2)°$. Crystal data for [Cu(oxoOEC•)][$SbCl_6$]: triclinic, space group $P\bar{1}$, $Z = 2$, $a = 13.063(1)$ Å, $b = 14.108(2)$ Å, $c = 11.486(2)$ Å, $\alpha = 93.77(3)°$, $\beta = 102.17(1)°$, $\gamma = 74.07(1)°$. The EPR spectrum of [Cu(oxoOEC•)][$SbCl_6$] in frozen dichloromethane at 77 K shows the characteristics of a dimeric copper(II) triplet state. Two broad, concentration-dependent near-IR "dimer bands" appear at 1285 and 1548 nm for [Cu(oxoOEC•)][$SbCl_6$]. Solid-state magnetic susceptibility measurements for [Cu(oxoOEC•)][$SbCl_6$] resulted in a large temperature dependence of the magnetic moments that can best be fit with a four-spin model. This model includes antiferromagnetic intermolecular copper−copper coupling ($2J_{Cu-Cu} = -70$ cm^{-1}), antiferromagnetic radical−radical coupling ($2J_{r-r} = -139$ cm^{-1}), and ferromagnetic intramolecular copper−radical coupling ($2J_{Cu-r} = 139$ cm^{-1}).

Introduction

We have been investigating the preparation and the molecular and electronic structures of various synthetic metalloporphyrin π-cation radical complexes. The study of magnetic interactions in π-cation radical metallooctaethylporphyrins is interesting mainly because of the importance of these or similar radicals in biological systems. For example, the oxidation of catalase and peroxidase by H_2O_2 is a two-electron process which leads to the formation of compound **I**, which is two oxidation equivalents above the resting ferric state. Compound **I** contains an iron(IV) center, with the additional oxidation equivalent residing on the porphyrin ring (a π-cation radical).[1] Catalase[2] and peroxidase[3−5] have very different catalytic activities, and model studies[6] have helped in the understanding of the tuning of the catalytic activities in these heme enzymes. The strength of intramolecular coupling between the metal center and the porphyrin π-cation radical clearly may be linked to structural differences important in determining the catalytic activities in these systems. However, detailed modeling of intramolecular coupling appropriate for systems such as the catalases and peroxidases[7,8] has been difficult since metalloporphyrin π-cation radical derivatives with alkyl substituents similar to naturally occurring systems are found to form dimeric systems. This dimeric structural feature is relatively easy to overcome in protein matrices, but is more difficult in isolated model systems.

Indeed, the formation of dimeric species is common in π-cation radical systems; relatively weak intermolecular (inter-ring) coupling of the unpaired π-cation radical electrons is observed in metallotetraphenylporphyrinate derivatives,[9−12] [M(TPP•)],[13] while several four- and five-coordinate metallooctaethylporphyrinate derivatives, [M(OEP•)], show exceptionally strong intermolecular coupling of π-cation radical dimers.[14−16] The differences in the magnitude of the spin coupling are correlated with inter-ring structure, with relatively large inter-ring coupling constants being associated with the formation of tight cofacial π−π dimers. In fact, the close π−π interactions in several [M(OEP•)] dimers has been shown to result in strong antiferromagnetic coupling between the spins of the two radicals,

* To whom correspondence should be addressed.
† University of Notre Dame.
§ Present address: Korean National University of Education, Chongwon.
‡ Knox College.

(1) Paeng, K.-J.; Kincaid, J. R. *J. Am. Chem. Soc.* **1988**, *110*, 7913.
(2) Corral, R. J. M.; Rodman, H. M.; Margolis, J.; Landau, B. R. *J. Biol. Chem.* **1974**, *249*, 3181.
(3) Meunier, B. *Biochimie* **1987**, *69*, 3.
(4) Augusto, O.; Schreiber, J.; Mason, R. P. *Biochem. Pharmacol.* **1988**, *37*, 2791.
(5) Ortiz de Montellano, P. R.; Grad, L. *Biochemistry* **1987**, *27*, 5310.
(6) Robert, A.; Loock, B.; Momenteau, M.; Meunier, B. *Inorg. Chem.* **1991**, *30*, 706.
(7) Schulz, C. E.; Rutter, R.; Sage, J. T.; Debrunner, P. G.; Hager, L. P. *Biochemistry* **1984**, *23*, 4743.
(8) Rutter, R.; Hager, L. P.; Dhonau, H.; Hendrich, M.; Valentine, M.; Debrunner, P. *Biochemistry* **1984**, *23*, 6809.
(9) Song, H.; Rath, N. P.; Reed, C. A.; Scheidt, W. R. *Inorg. Chem.* **1989**, *28*, 1839.
(10) Erler, B. S.; Scholz, W. F.; Lee, Y. J.; Scheidt, W. R.; Reed, C. A. *J. Am. Chem. Soc.* **1987**, *109*, 2644.
(11) Gans, P.; Buisson, G.; Duee, E.; Marchon, J.-C.; Erler, B. S.; Scholz, W. F.; Reed, C. A. *J. Am. Chem. Soc.* **1986**, *108*, 1223.
(12) Barkigia, K. M.; Spaulding, L. D.; Fajer, J. *Inorg. Chem.* **1983**, *22*, 349.

10.1021/ic9903026 CCC: $18.00
Published on Web 08/26/1999

yielding diamagnetic pairs.[14] In the [M(OEP•)] radical cations the two rings are effectively eclipsed; these systems are also characterized by the absence of any significant lateral shift between two porphyrin rings and a large enthalpy of dimerization (∼15−18 kcal/mol).[17]

When a metalloporphyrin π-cation radical contains a paramagnetic metal center, there exists the possibility of *intra*molecular spin coupling between the unpaired electrons on the metal and the unpaired electron on the porphyrin ring. Two distinct intramolecular coupling mechanisms have been found; the nature of the coupling (ferro- or antiferromagnetic) is dependent on the conformation of the porphyrin core.[9,14,18−21] Ferromagnetic coupling exists when the porphyrin ring is essentially planar and approximates D_{4h} symmetry; the partially filled metal orbitals are orthogonal to the porphyrin π-cation radical orbitals. Antiferromagnetic coupling arises in complexes containing distorted macrocycles; these are typically lower symmetry systems where the magnetic orbitals of the metal and ligand are allowed by symmetry to overlap. However, the existence of synthetic [M(OEP•)] radical cations as tightly-coupled diamagnetic pairs has precluded the detailed study of intramolecular interactions in these systems. Attempts at determining the intramolecular coupling component in π-cation radical systems containing a paramagnetic copper(II) center have only been successful in systems containing peripheral substituents that are sterically demanding.[22−24] The introduction of bulky substituents at the periphery presumably prevents dimerization.

Cases where both intra- and intermolecular spin coupling can be significant are less well understood. For example, the [Cu(OEP•)]$^+$ and [Cu(OEC•)]$^+$ radical complexes show Cu···Cu triplet EPR spectra[25,26] with no evidence for unpaired π-cation radical electrons in their EPR or bulk magnetic susceptibility. These systems can best be described as pairwise interacting complexes. Similarly, in the six-coordinate complex, [VO(OH$_2$)(OEP•)]$SbCl_6$, where there is only an edge-over-edge overlap between porphyrin rings,[21] the magnetic data are best described as having two components: intramolecular ferromagnetic coupling and relatively strong intermolecular antiferromagnetic coupling.

Although many biologically active heme proteins contain the parent porphyrin prosthetic group, there is an increasing body of evidence which shows that the generic class of hydroporphyrins (porphyrin systems in which one or more $\beta-\beta$ pyrrole bonds are saturated) displays a wide range of functions in biological systems.[27−51] More specifically, heme d_1, which consists of an unusual dioxoisobacteriochlorin,[40−44,48] is known be involved in the function of bacterial nitrite reductases. Thus, metallo-β-oxochlorin derivatives can be viewed as model complexes for protein structures which contain heme d_1. In this paper we present the preparation and complete characterization (structural, electronic, and magnetic) of two new copper(II)(oxooctaethylchlorin) (oxoOEC) complexes. Our synthetic strategy involves the use of the *gem*-diethyl group of the oxochlorin ring to prevent the formation of tight cofacial $\pi-\pi$ dimers that is characteristic of all four- and five-coordinate metallooctaethylporphyrinate π-cation radicals. As mentioned above, a relative of this class of porphyrins, the dioxoisobacteriochlorin (dioxoOEiBC), is now known to be the prosthetic group of the noncovalently bound heme d_1 of the bacterial nitrite reductase. To date only one [M(oxoOEC)] complex, neutral [Ni(oxoOEC)],

(13) Abbreviations used in this paper: OEP, octaethylporphyrin; (OEP•), the π-cation radical of OEP; TPP, tetraphenylporphyrin; OETPP, octaethyltetraphenylporphyrin; TMTMP, 2,7,12,17-tetramethyl-3,8,-13,18-tetramesitylporphyrin; OEC, octaethylchlorin; oxoOEC (oxooctaethylchlorin), 3,3,7,8,12,13,17,18-octaethyl-(3*H*)-porphin-2-onato-(2−); (oxoOEC•), the π-cation radical of oxoOEC; dioxoOEiBC (dioxooctaethylisobacteriochlorin), 3,3,8,8,12,13,17,18-octaethyl-(3*H*,8*H*)-porphine-2,7-dionato; trioxoOEHP (trioxooctaethylhexahydroporphyrin), 3,3,7,8,12,12,18,18-octaethyl-(3*H*,12*H*,18*H*)-porphine-2,13,17-trionato; [Cu(rhodochlorin)], 3^1,3^2-didehydrorhodochlorinato-15-formic acid (trimethyl ester)copper(II); [Cu(*n*-PrP)], copper(II) $\alpha,\beta,\gamma,\delta$-tetra-*n*-propylporphine; SQUID, superconducting quantum interference device.

(14) Song, H.; Orosz, R. D.; Reed, C. A.; Scheidt, W. R. *Inorg. Chem.* **1990**, *29*, 4274.
(15) Barkigia, K. M.; Renner, M. W.; Fajer, J. *J. Phys. Chem. B* **1997**, *101*, 8398.
(16) Schulz, C. E.; Song, H.; Mislanker, A.; Orosz, R. D.; Reed, C. A.; Debrunner, P. G.; Scheidt, W. R. *Inorg. Chem.* **1997**, *36*, 406.
(17) Fuhrhop, J. H.; Wasser, P.; Riesner, D.; Mauzerall, D. *J. Am. Chem. Soc.* **1972**, *94*, 7996.
(18) Scholz, W. F.; Reed, C. A.; Lee, Y. J.; Scheidt, W. R.; Lang, G. *J. Am. Chem. Soc.* **1982**, *104*, 6791.
(19) Gans, P.; Buisson, G.; Duee, E.; Marchon, J.-C.; Erler, B. S.; Scholz, W. F.; Reed, C. A. *J. Am. Chem. Soc.* **1986**, *108*, 1223.
(20) Song, H.; Reed, C. A.; Scheidt, W. R. *J. Am. Chem. Soc.* **1989**, *111*, 6865.
(21) Schulz, C. E.; Song, H.; Lee, Y. J.; Mondal, J. U.; Mohanrao, K.; Reed, C. A.; Walker, F. A.; Scheidt, W. R. *J. Am. Chem. Soc.* **1994**, *116*, 7196.
(22) Renner, M. W.; Barkigia, K. M.; Zhang, Y.; Medforth, C. J.; Smith, K. M.; Fajer, J. *J. Am. Chem. Soc.* **1994**, *116*, 8562.
(23) Renner, M. W.; Barkigia, K. M.; Fajer, J. *Inorg. Chim. Acta* **1997**, *263*, 181.
(24) Fujii, H. *Inorg. Chem.* **1993**, *32*, 875.
(25) Godziela, G. M.; Goff, H. M. *J. Am. Chem. Soc.* **1986**, *108*, 2237.
(26) Mengersen, C.; Subramanian, J.; Fuhrhop, J.-H. *Mol. Phys.* **1976**, *32*, 893.
(27) Barkigia, K. M.; Chantranupong, L.; Smith, K. M.; Fajer, J. *J. Am. Chem. Soc.* **1988**, *110*, 7566.
(28) Strauss, S. H.; Silver, M. E.; Long, K. M.; Thompson, R. G.; Hudgens, R. A.; Spartalian, K.; Ibers, J. A. *J. Am. Chem. Soc.* **1985**, *107*, 4207.
(29) Barkigia, K. M.; Fajer, J.; Chang, C. K.; Williams, G. J. B. *J. Am. Chem. Soc.* **1982**, *104*, 315.
(30) Barkigia, K. M.; Chang, C. K.; Fajer, J. *J. Am. Chem. Soc.* **1991**, *113*, 7445.
(31) Renner, M. W.; Furenlid, L. R.; Barkigia, K. M.; Forman, A.; Shim, H.-K.; Simpson, D. J.; Smith, K. M.; Fajer, J. *J. Am. Chem. Soc.* **1991**, *113*, 6891.
(32) Strauss, S. H.; Pawlik, M. J.; Skowyra, J.; Kennedy, J. R.; Anderson, O. P.; Spartalian, K.; Dye, J. L. *Inorg. Chem.* **1987**, *26*, 724.
(33) Suh, M. P.; Swepston, P. N.; Ibers, J. A. *J. Am. Chem. Soc.* **1984**, *106*, 5164.
(34) Barkigia, K. M.; Fajer, J.; Spaulding, L. D.; Williams, G. J. B. *J. Am. Chem. Soc.* **1981**, *103*, 176.
(35) Walling, C. *J. Am. Chem. Soc.* **1980**, *102*, 6852.
(36) Spaulding, L. D.; Andrews, L. C.; Williams, G. J. B. *J. Am. Chem. Soc.* **1977**, *99*, 6918.
(37) Stolzenberg, A. M.; Simerly, S. W.; Steffey, B. D.; Haymond, G. S. *J. Am. Chem. Soc.* **1997**, *119*, 11843.
(38) Barkigia, K. M.; Miura, M.; Thompson, M. A.; Fajer, J. *Inorg. Chem.* **1991**, *30*, 2233.
(39) Vasudevan, J.; Stibrany, R. T.; Bumby, J.; Knapp, S.; Potenza, J. A.; Emge, T. J.; Schugar, H. J. *J. Am. Chem. Soc.* **1996**, *118*, 11676.
(40) Chang, C. K.; Timkovich, R.; Wu, W. *Biochemistry* **1986**, *25*, 8447.
(41) Wu, W.; Chang, C. K. *J. Am. Chem. Soc.* **1987**, *109*, 3149.
(42) Chang, C. K.; Wu, W. *J. Biol. Chem.* **1986**, *261*, 8593.
(43) Weeg-Aerssens, E.; Wu, W.; Ye, R. W.; Tiedje, J. M.; Chang, C. K. *J. Biol. Chem.* **1991**, *266*, 7496.
(44) Williams, P. A.; Fulop, V.; Garman, E. F.; Saunders, N. F. W.; Ferguson, S. J.; Hajdu, J. *Nature* **1997**, *389*, 406.
(45) Stolzenberg, A. M.; Glazer, P. A.; Foxman, B. M. *Inorg. Chem.* **1986**, *25*, 983.
(46) Connick, P. A.; Haller, K. J.; Macor, K. A. *Inorg. Chem.* **1993**, *32*, 3256.
(47) Chang, C. K.; Barkigia, K. M.; Hanson, L. K.; Fajer, J. *J. Am. Chem. Soc.* **1986**, *108*, 1352.
(48) Barkigia, K. M.; Chang, C. K.; Fajer, J.; Renner, M. W. *J. Am. Chem. Soc.* **1992**, *114*, 1701.
(49) Senge, M. O.; Ruhlandt-Senge, K.; Lee, S.-J.; Smith, K. M. *Z. Naturforsch., Teil B* **1995**, *50*, 969.
(50) Senge, M. O.; Kallisch, W. W.; Ruhlandt-Senge, K. *J. Chem. Soc., Chem. Commun.* **1996**, 2149.
(51) Jaquinod, L.; Gros, C.; Khoury, R. G.; Smith, K. M. *J. Chem. Soc., Chem. Commun.* **1996**, 2581.

has been structurally characterized.[45,46] We report here the structural characterization of the neutral [Cu(oxoOEC)] complex and the first structurally characterized π-cation radical derivative of this special class of compounds, [Cu(oxoOEC$^{\bullet}$)][$SbCl_6$].

Experimental Section

General Information. H_2OEP was synthesized by literature methods.[52] Copper(II) acetate was from J. T. Baker, and tris(4-bromophenyl)-aminium hexachloroantimonate was purchased from Aldrich. Dichloromethane and hexanes were distilled under argon from CaH_2 and sodium/benzophenone, respectively. Reactions involving the π-cation radical were performed under argon atmosphere with oven-dried Schlenkware and cannula techniques.

Synthesis of [Cu(oxoOEC)]. H_2(oxoOEC) was synthesized by modified literature procedures.[53−55] Insertion of copper metal into H_2-(oxoOEC) was accomplished by the reaction of the free base and copper(II) acetate in DMF.[56] Crystals of [Cu(oxoOEC)] were grown at room temperature by vapor diffusion of pentane into a dichloromethane solution of [Cu(oxoOEC)]. UV−vis (CH_2Cl_2 solution): λ_{max} 414 (Soret), 506, 569, 618 nm. IR(KBr): ν(CO) 1710 cm^{-1}.

Synthesis of [Cu(oxoOEC$^{\bullet}$)][$SbCl_6$]. [Cu(oxoOEC)] (25 mg, 0.040 mmol) and tris(4-bromophenyl)aminium hexachloroantimonate (34 mg, 0.042 mmol) were placed in a 100-mL Schlenk flask and dried for 30 min under vacuum. After dichloromethane was added, the brown solution was stirred for 10 min. Hexane (nonsolvent) was added, the mixture was filtered, and the brown solid was dried in vacuo. Suitable crystals of [Cu(oxoOEC$^{\bullet}$)][$SbCl_6$] were obtained from the slow diffusion of hexanes into a chloroform solution of [Cu(oxoOEC$^{\bullet}$)][$SbCl_6$]. UV/vis/near-IR (CH_2Cl_2): λ_{max} 393 (Soret), 491, 700, 1285, 1548 nm. IR-(KBr): ν(CO) 1730 cm^{-1}, ν(SbCl) 344 cm^{-1}.

X-ray Structure Determinations. Single crystals of [Cu(oxoOEC)] and [Cu(oxoOEC$^{\bullet}$)][$SbCl_6$] were examined on a Nonius FAST area-detector diffractometer at 127 K with a Mo rotating anode source (λ = 0.710 73 Å). Detailed methods and procedures for small molecule X-ray data collection with the FAST system have been described elsewhere.[57] Intensity data were corrected for Lorentz and polarization effects.

The structure of [Cu(oxoOEC)] was solved by the Patterson method, and the structure of [Cu(oxoOEC$^{\bullet}$)][$SbCl_6$] was solved by direct methods with the SHELXS-86 program. The [Cu(oxoOEC)] structure was refined by a least-squares procedure based on F, and the [Cu-(oxoOEC$^{\bullet}$)][$SbCl_6$] structure was refined against F^2 with the SHELXL program.[58] An absorption correction was applied at the final stages of the structure determination of [Cu(oxoOEC$^{\bullet}$)][$SbCl_6$]. All hydrogen atoms, except those attached to the disordered carbon atoms of [Cu-(oxoOEC$^{\bullet}$)][$SbCl_6$], were idealized with the standard SHELXL idealization methods and were included in subsequent least-square refinement cycles. Brief crystallographic details for both structures are given in Table 1.

Physical Characterization. UV/vis/near-IR spectra were recorded on a Perkin-Elmer Lambda 19 UV/vis/near-IR spectrometer. IR spectra were recorded on a Perkin-Elmer 883 spectrometer. EPR spectra were obtained at 77 K on a Varian E-12 spectrometer operating at X-band. The solution spectrum of [Cu(oxoOEC$^{\bullet}$)][$SbCl_6$] was measured near the concentration limit (~3.6×10^{-3} M). The solid-state spectrum was measured on a finely powdered sample. Magnetic susceptibility measurements were obtained on ground samples in the solid state over the temperature range 6−300 K on a Quantum Design MPMS SQUID susceptometer. Measurements at two fields (2 and 20 kG) showed that no ferromagnetic impurities were present; duplicate measurements ensured reproducibility among different sample preparations. χ_M was corrected for the underlying porphyrin ligand diamagnetism according to previous experimentally observed values;[59] all remaining diamagnetic contributions (χ_{dia}) were calculated using Pascal's constants.[60,61] All measurements included a correction for the diamagnetic sample holder.

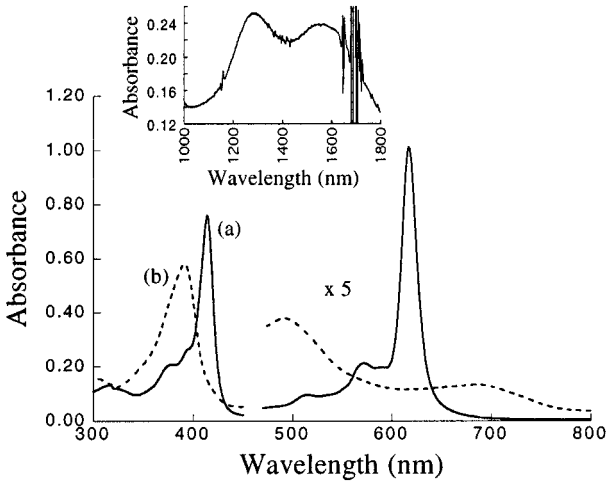

Figure 1. UV−visible spectra of (a) [Cu(oxoOEC)] (3.85×10^{-5} M) and (b) [Cu(oxoOEC$^{\bullet}$)][$SbCl_6$] (3.71×10^{-5} M) in CH_2Cl_2. The spectra on the left side of the plot were collected using a 1 mm cell; the spectra on the right were collected using a 10 mm cell. The upper inset shows the near-IR bands of [Cu(oxoOEC$^{\bullet}$)][$SbCl_6$] (1.84×10^{-3} M).

Table 1. Crystallographic Details for [Cu(oxoOEC)] and [Cu(oxoOEC$^{\bullet}$)][$SbCl_6$]

molecule	[Cu(oxoOEC)]	[Cu(oxoOEC$^{\bullet}$)][$SbCl_6$]
chemical formula	$CuN_4C_{36}O_1H_{44}$	$CuN_4C_{36}O_1H_{44}SbCl_6$
fw, amu	612.32	946.79
a, Å	38.404 (8)	13.063 (1)
b, Å	14.692 (6)	14.108 (2)
c, Å	16.977 (11)	11.486 (1)
α, deg	90.00	93.77 (3)
β, deg	101.456 (18)	102.17 (1)
γ, deg	90.00	74.07 (1)
V, Å^3	9388 (12)	1989.7 (4)
Z	12	2
space group	$C2/c$ (no. 15)	$P\bar{1}$ (no. 2)
temperature, K	127(1)	127(2)
radiation ($\bar{\lambda}$, Å)	Mo Kα (0.71073)	Mo Kα (0.71073)
D_c, g/cm^3	1.300	1.572
μ, mm^{-1}	0.7313	1.650
R indices [$I > 2\sigma(I)$]	$R_1 = 0.064$, $wR_2 = 0.072$	$R_1 = 0.0412$, $wR_2 = 0.1027$
R indices (all data)		$R_1 = 0.0480$, $wR_2 = 0.1072$

Results

The oxidation of [Cu(oxoOEC)] with tris(4-bromophenyl)-aminium hexachloroantimonate results in the formation of the π-cation radical, [Cu(oxoOEC$^{\bullet}$)][$SbCl_6$]. The electronic spectrum of the oxidized complex (Figure 1) has a blue-shifted and broadened Soret band, the bands in the visible region have decreased in intensity, and two new broad, concentration-dependent near-IR bands appear at 1285 and 1548 nm. In the

(52) Sessler, J. *Org. Synth.* **1992**, *70*, 68.
(53) Inhoffen, H. H.; Nolte, W. *Liebigs Ann. Chem.* **1969**, *725*, 167.
(54) Chang, C. K. *Biochemistry* **1980**, *19*, 1971.
(55) Chang, C. K.; Sotiriou, Chariklia *J. Org. Chem.* **1985**, *50*, 4989.
(56) Adler, A. D.; Longo, F. R.; Kampas, F.; Kim, J. *J. Inorg. Nucl. Chem.* **1970**, *32*, 2443.
(57) Scheidt, W. R.; Turowska-Tyrk, I. *Inorg. Chem.* **1994**, *33*, 1314.
(58) Programs used in this study included SHELXS-86 (Sheldrick, G. M. *Acta Crystallogr., Sect. A* **1990**, *A46*, 467), SHELXL-93 (Sheldrick, G. M. *J. Appl. Crystallogr.*, in preparation), and local modifications of ORTEP (Johnson, C. K. *ORTEP: A Fortran Thermal-Ellipsoid Plot Program For Crystal Structure Illustrations*; Oak Ridge National Laboratory: Oak Ridge, TN, 1970). Scattering factors were taken from *International Tables for Crystallography*; Wilson, A. J. C., Ed.; Kluwer Academic Publishers: Dordrecht, 1992; Vol. C.
(59) Sutter, T. P. G.; Hambright, P.; Thorpe, A. N.; Quoc, N. *Inorg. Chim. Acta* **1992**, *195*, 131.
(60) Selwood, P. W. *Magnetochemistry*; Interscience: New York, 1956; Chapter 2.
(61) Earnshaw, A. *Introduction to Magnetochemistry*; Academic: London, 1968; Chapter 1.

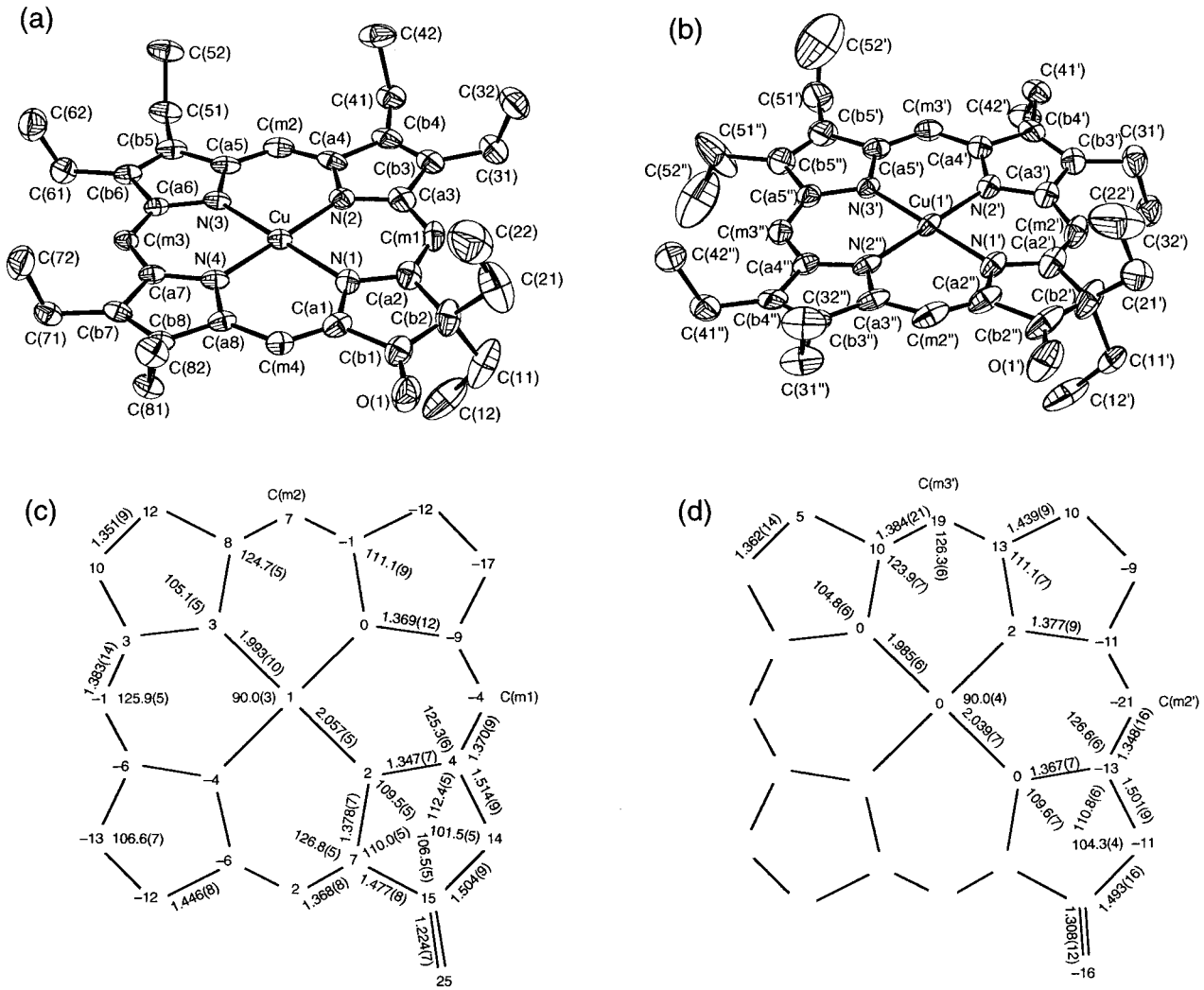

Figure 2. Labeled ORTEP diagrams of [Cu(oxoOEC)] for the general position (a) and the special position (b) molecule. The special position molecule has a required 2-fold axis of symmetry that lies in the macrocyclic plane and bisects the saturated $C_\beta-C_\beta$ bond (Cb2′−Cb2″). Thermal ellipsoids are drawn to illustrate 50% probability surfaces. Formal diagrams giving the perpendicular displacements of each atom from the 24-atom mean planes (in Å × 10^2) of [Cu(oxoOEC)] for the general position (c) and the special position (d) molecule. All bond lengths and angles of the pyrrolinone ring are shown. The remaining bond lengths and angles are averages of those for the pyrrole rings. The estimated standard uncertainties are shown in parentheses; the uncertainties of the bond parameters reported for the pyrrolinone ring are those of the individual bond lengths and angles, while the numbers in parentheses of the remaining bond parameters represent the esd's calculated for the averaged bond lengths and angles of the pyrrole rings.

infrared, the carbonyl band at 1710 cm^{-1} for the neutral compound, [Cu(oxoOEC)], shifts to 1730 cm^{-1} upon formation of the π-cation radical, [Cu(oxoOEC•)][$SbCl_6$]. A new IR band similar to the radical marker band in OEP π-cation radical derivatives is seen at 1560 cm^{-1}.

The molecular structures of [Cu(oxoOEC)] and the one-electron oxidation product, [Cu(oxoOEC•)][$SbCl_6$], have been determined by X-ray crystallography. [Cu(oxoOEC)] has two crystallographically distinct molecules, one at a general position ([Cu(oxoOEC)]-gen) and a second at a special position ([Cu-(oxoOEC)]-spe). The special position molecule has a required 2-fold axis of symmetry that lies in the macrocyclic plane and bisects the saturated $C_\beta-C_\beta$, bond. Figure 2 shows labeled ORTEP diagrams and formal diagrams giving the perpendicular displacements of each atom from the 24-atom mean plane for [Cu(oxoOEC)]-gen and [Cu(oxoOEC)]-spe. Figure 3 shows a labeled ORTEP diagram and a formal diagram giving the perpendicular displacements of each atom from the 24-atom mean plane for the π-cation radical, [Cu(oxoOEC•)][$SbCl_6$]. Table 2 contains selected bond distances and angles for [Cu-(oxoOEC)]-gen, [Cu(oxoOEC)]-spe, and [Cu(oxoOEC•)][$SbCl_6$]. Final atomic coordinates are included in the Supporting Information.

Individual bond lengths and angles for the pyrrolinone[62] ring and averaged bond lengths for the pyrrole rings are displayed in Figures 2c, 2d, and 3b. The estimated standard uncertainties are shown in parentheses; the uncertainties of the bond parameters reported for the pyrrolinone ring are those of the individual bond lengths and angles, while the numbers in parentheses of the remaining bond parameters represent the esd's calculated for the averaged bond lengths and angles of the pyrrole rings.

Edge-on and top-down views of the closest interacting "dimeric" pairs of [Cu(oxoOEC)]-gen and [Cu(oxoOEC)]-spe are shown in Figure 4. Figure 5 shows the corresponding views for [Cu(oxoOEC•)][$SbCl_6$]. The two rings of each dimer are related by an inversion center. The geometry (Cu···Cu distance,

(62) Other terms commonly used to describe the reduced ring that contains a carbonyl group include "pyrrolidinone," "pyrrolidine," and "pyrroline."

Ct···Ct distance, mean plane separation, and lateral shift) for each dimeric unit is summarized in Table 4.

The EPR spectrum of [Cu(oxoOEC•)][$SbCl_6$] in frozen dichloromethane at 77 K is shown in Figure 6. The EPR spectrum shows three major signals at 1550, 3000, and 3500 G. The EPR spectrum resembles those reported for the [Cu(OEP•)]$^+$ and [Cu(OEC•)]$^+$ π-cation radicals.[25,26]

Temperature-dependent (6−300 K) magnetic susceptibility measurements were carried out for [Cu(oxoOEC)] and [Cu(oxoOEC•)][$SbCl_6$]. [Cu(oxoOEC)] has a room temperature magnetic moment of 1.90 μ_B and shows no temperature dependence of the magnetic moment (see Figure S1, Supporting Information). In contrast, [Cu(oxoOEC•)][$SbCl_6$] has a magnetic moment with a large temperature dependence. Figure 7 shows the temperature dependence of the magnetic moment for [Cu(oxoOEC•)][$SbCl_6$].

Discussion

Optical and IR spectral data indicate that the oxidation of [Cu(oxoOEC)] results in the formation of a π-cation radical. In the UV, the Soret band blue shifts and broadens upon oxidation; the bands in the visible region decrease in intensity upon oxidation (see Figure 1). Two broad, concentration-dependent near-IR bands are observed at 1285 and 1548 nm; the neutral (unoxidized) [Cu(oxoOEC)] complex does not absorb in either of these regions. These two bands (inset, Figure 1) show the same concentration dependence and were studied over the concentration range 3.65×10^{-3} to 1.16×10^{-4} M. The band intensity decreases such that there is no longer clear evidence for absorption maxima below $\sim 2.0 \times 10^{-4}$ M. Such near-IR bands have been observed in metallooctaethylporphyrin π-cation radicals,[63−65] where they all result from the formation of dimeric π-cation radical species, [M(OEP•)]$_2^{2+}$. These near-IR "dimer bands" are modestly metal dependent and can be counteranion dependent.[63] Absorption maxima are found in the region 900−960 nm for nickel, copper, palladium, and zinc octaethylporphyrin π-cation radicals; the vanadyl complex[21] has a red-shifted near-IR band at 1375 nm. Thus, the near-IR band found in [Cu(oxoOEC•)]$_2^{2+}$ at 1285 nm is red-shifted when compared to [Cu(OEP•)]$_2^{2+}$ and approaches the absorption maximum found in the vanadyl octaethylporphyrin π-cation radical.

[Cu(oxoOEC•)][$SbCl_6$] shows a π-cation radical IR marker band at $\sim$1560 cm^{-1}. This band is similar to the π-cation radical IR marker bands found in octaethylporphyrinate and β-alkyl-substituted porphyrinate π-cation radical derivatives ($\sim$1550 cm^{-1}); *meso*-tetraaryl substituted porphyrin π-cation radicals exhibit diagnostic π-cation radical IR marker bands at $\sim$1280 cm^{-1}.[66,67] Upon oxidation of [Cu(oxoOEC)], the carbonyl band in the infrared shifts from 1710 to 1730 cm^{-1}. This large oxidation-induced shift of the carbonyl band indicates that the oxidation of [Cu(oxoOEC)] accompanies a significant change of the electronic structure of the macrocycle. More specifically, the increase in energy of the carbonyl band upon oxidation is consistent with the removal of electron density from the porphyrin ring, forming the π-cation radical.

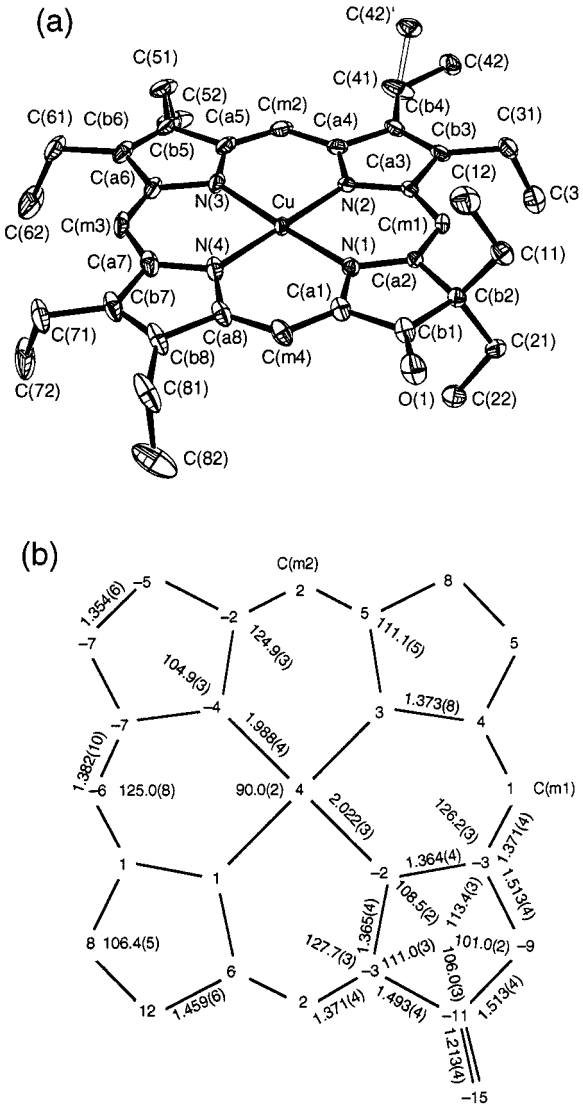

Figure 3. (a) Labeled ORTEP diagram for the [Cu(oxoOEC•)][$SbCl_6$] radical. Thermal ellipsoids are drawn to illustrate 50% probability surfaces. (b) Formal diagram giving the perpendicular displacements of each atom from the 24-atom mean plane (in Å $\times$ 10^2) for [Cu(oxoOEC•)][$SbCl_6$]. All bond lengths and angles of the pyrrolinone ring are shown. The remaining bond lengths and angles are averages of those for the pyrrole rings. The estimated standard uncertainties are shown in parentheses; the uncertainties of the bond parameters reported for the pyrrolinone ring are those of the individual bond lengths and angles, while the numbers in parentheses of the remaining bond parameters represent the esd's calculated for the averaged bond lengths and angles of the pyrrole rings.

The crystal structures of [Cu(oxoOEC)] and [Cu(oxoOEC•)][$SbCl_6$] have been determined; this allows a comparison of the effects of oxidation on both the structural features and the magnetic properties. In the crystal, there are two crystallographically distinct molecules of [Cu(oxoOEC)] that have small differences in core conformation. Two types of Cu−N distances are observed in each porphyrin ring: "short" Cu−N distances (1.981(5)−1.999(4) Å) to the pyrroles and "long" Cu−N distances (2.057(5), 2.039(7) Å) to the pyrrolinone ring. The short distances are typical of Cu−N bond lengths found in planar copper porphyrinates,[68−74] while the long distances are typical

(63) Brancato-Buentello, K. E.; Kang, S.-J.; Scheidt, W. R. *J. Am. Chem. Soc.* **1997**, *119*, 2839.
(64) Fuhrhop, J. H.; Wasser, P.; Riesner, D.; Mauzerall, D. *J. Am. Chem. Soc.* **1972**, *94*, 7996.
(65) Fajer, J.; Borg, D. C.; Forman, A.; Dolphin, D.; Felton, R. H. *J. Am. Chem. Soc.* **1970**, *92*, 3451.
(66) Hu, S.; Spiro, T. G. *J. Am. Chem. Soc.* **1993**, *115*, 12029.
(67) Shimomura, E. T.; Phillippi, M. A.; Goff, H. M.; Scholz, W. F.; Reed, C. A. *J. Am. Chem. Soc.* **1981**, *103*, 6778.
(68) Pak, R.; Scheidt, W. R. *Acta Crystallogr., Sect. C* **1991**, *C47*, 431.
(69) Moustakali, I.; Tulinsky, A. *J. Am. Chem. Soc.* **1973**, *95*, 6811.
(70) Scheidt, W. R.; Lee, Y. J. *Struct. Bonding (Berlin)* **1987**, *64*, 1.

Table 2. Summary of Bond Lengths and Angles for Cu(oxoOEC) Complexes

	[Cu(oxoOEC)]-gen	[Cu(oxoOEC)]-spe	[Cu(oxoOEC•)][$SbCl_6$]
	Bond Lengths (Å)		
Cu−N(1)	2.057(5)	2.039(7)	2.022(3)
Cu−N(2)	1.981(5)	1.985(5)	1.985(3)
Cu−N(3)	1.999(4)	1.984(6)	1.988(3)
Cu−N(4)	1.998(5)		1.992(3)
N(1)−C(a1)	1.378(7)		1.365(4)
N(1)−C(a2)	1.347(7)	1.367(7)	1.364(4)
N(2)−C(a3)	1.350(8)	1.367(7)	1.365(4)
N(2)−C(a4)	1.384(8)	1.382(7)	1.377(4)
N(3)−C(a5)	1.362(6)	1.383(7)	1.369(5)
N(3)−C(a6)	1.374(7)		1.386(4)
N(4)−C(a7)	1.374(7)		1.376(4)
N(4)−C(a8)	1.371(7)		1.366(5)
C(a1)−C(b1)	1.477(8)		1.493(4)
C(a2)−C(b2)	1.514(9)	1.501(9)	1.513(4)
C(a3)−C(b3)	1.443(8)	1.433(9)	1.453(5)
C(a4)−C(b4)	1.450(8)	1.437(8)	1.463(5)
C(a5)−C(b5)	1.438(8)	1.447(8)	1.465(4)
C(a6)−C(b6)	1.448(7)		1.454(5)
C(a7)−C(b7)	1.450(7)		1.455(6)
C(a8)−C(b8)	1.446(7)		1.465(4)
C(b1)−C(b2)	1.504(9)	1.493(16)	1.513(4)
C(b3)−C(b4)	1.351(9)	1.367(8)	1.360(4)
C(b5)−C(b6)	1.360(8)	1.357(14)	1.352(6)
C(b7)−C(b8)	1.342(8)		1.351(6)
C(b)−O	1.224(7)	1.308(12)	1.213(4)
	Bond Angles (deg)		
N(1)−Cu−N(2)	89.51(19)	89.74(13)	89.84(10)
N(2)−Cu−N(3)	90.05(19)	90.26(13)	90.05(12)
N(1)−Cu−N(4)	90.26(19)		89.78(11)
N(3)−Cu−N(4)	90.23(18)		90.26(12)
N(1)−Cu−N(3)	178.77(18)	180.00	176.00(10)
C(a1)−N(1)−C(a2)	109.5(5)	109.6(7)	108.5(2)
C(a3)−N(2)−C(a4)	104.7(5)	104.7(5)	104.6(3)
C(a5)−N(3)−C(a6)	105.4(5)	104.8(6)	105.2(3)
C(a7)−N(4)−C(a8)	105.2(4)		105.0(3)
N(1)−C(a1)−C(b1)	110.0(5)		111.0(3)
N(1)−C(a2)−C(b2)	112.4(5)	110.8(6)	113.4(3)
N(2)−C(a3)−C(b3)	112.4(6)	111.9(5)	112.0(3)
N(2)−C(a4)−C(b4)	110.2(6)	110.6(5)	111.1(3)
N(3)−C(a5)−C(b5)	110.8(5)	110.9(6)	111.0(3)
N(3)−C(a6)−C(b6)	111.9(5)		110.5(3)
N(4)−C(a7)−C(b7)	110.1(5)		110.8(3)
N(4)−C(a8)−C(b8)	111.0(5)		111.4(3)
C(a1)−C(b1)−C(b2)	106.5(5)		106.0(3)
C(a2)−C(b2)−C(bl)	101.5(5)	104.3(4)	101.0(2)
C(a3)−C(b3)−C(b4)	105.7(5)	105.9(5)	106.1(3)
C(a4)−C(b4)−C(b3)	107.0(5)	106.8(5)	106.1(3)
C(a5)−C(b5)−C(b6)	107.2(5)	106.7(4)	106.2(3)
C(a6)−C(b6)−C(b5)	105.7(5)		107.1(3)
C(a7)−C(b7)−C(b8)	107.3(5)		107.0(3)
C(a8)−C(b8)−C(b7)	106.4(5)		105.8(3)

of Cu−N distances found in the reduced rings of [Cu(dioxoOEiBC][47] and in copper hydroporphyrinates[49−51] (see Table 3). The small differences in the average Cu−N bond lengths between [Cu(oxoOEC)]-gen ($Cu-N_{pyrrole}$ = 1.993(10), $Cu-N_{pyrrolinone}$ = 2.057(5)) and [Cu(oxoOEC)]-spe ($Cu-N_{pyrrole}$ = 1.985(6), $Cu-N_{pyrrolinone}$ = 2.039(7)) are the result of changes in macrocyclic conformation; the general position molecule of [Cu(oxoOEC)] has a small but real S_4-saddled conformation, while the special position molecule is S_4-ruffled. It is expected that the S_4-saddled general position molecule will have slightly longer Cu−N bond lengths as the nitrogens have moved slightly out of the macrocyclic plane. This small variation in metal-to-nitrogen bond lengths as a result of ring conformation has also been seen in [Ni(oxoOEC)].[45,46] After oxidation to [Cu(oxoOEC•)][$SbCl_6$], the "long" Cu−N distance to the pyrrolinone ring decreases from 2.057(5) to 2.022(3) Å, while the average "short" Cu−N distance (1.993(10) and 1.987(5) Å) to the pyrrole rings stays the same. Thus, the Cu−N bond to the pyrrolinone ring is affected more than the Cu−N bond to the pyrrole rings upon removal of an electron from the macrocycle.

The pyrrolinone rings of [Cu(oxoOEC)] and [Cu(oxoOEC•)][$SbCl_6$] have lengthened $C_\beta-C_\beta$ bonds and widened $C_\alpha-N-C_\alpha$ angles as expected for a reduced ring. The $C_\alpha-C_\beta$ bond containing the carbonyl group is shorter than the $C_\alpha-C_\beta$ bond containing the *gem*-diethyl group ($C_\alpha-C_{\beta(carbonyl)}$ = 1.447(8) Å vs $C_\alpha-C_{\beta(gem-diethyl)}$ = 1.514(9) Å); the difference suggests

(71) Senge, M. O.; Medforth, C. J.; Sparks, L. D.; Shelnutt, J. A.; Smith, K. A. *Inorg. Chem.* **1993**, *32*, 1716.
(72) Byrn, M. P.; Curtis, C. J.; Hsiou, Y.; Khan, S. I.; Sawin, P. A.; Tendick, S. K.; Terzis, A.; Strouse, C. E. *J. Am. Chem. Soc.* **1993**, *115*, 9480.
(73) Byrn, M. P.; Curtis, C. J.; Goldberg, I.; Hsiou, Y.; Khan, S. I.; Sawin, P. A.; Tendick, S. K.; Strouse, C. E. *J. Am. Chem. Soc.* **1991**, *113*, 6549.
(74) Kumar, R. K.; Balasubramanian, S.; Goldberg, I. *Inorg. Chem.* **1998**, *37*, 541.

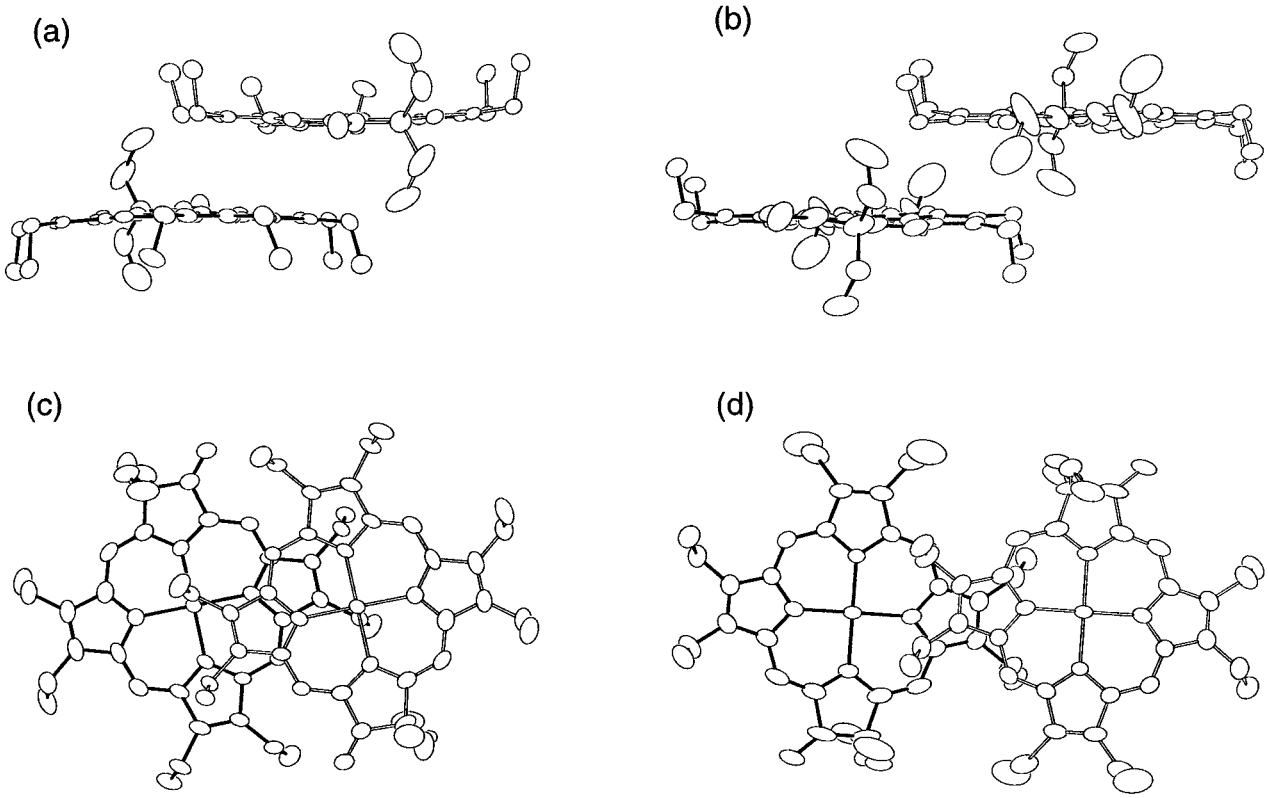

Figure 4. Edge-on views of the closest inversion related dimeric units of (a) [Cu(oxoOEC)]-gen and (b) [Cu(oxoOEC)]-spe. Top-down views of the dimeric units of (c) [Cu(oxoOEC)]-gen and (d) [Cu(oxoOEC)]-spe.

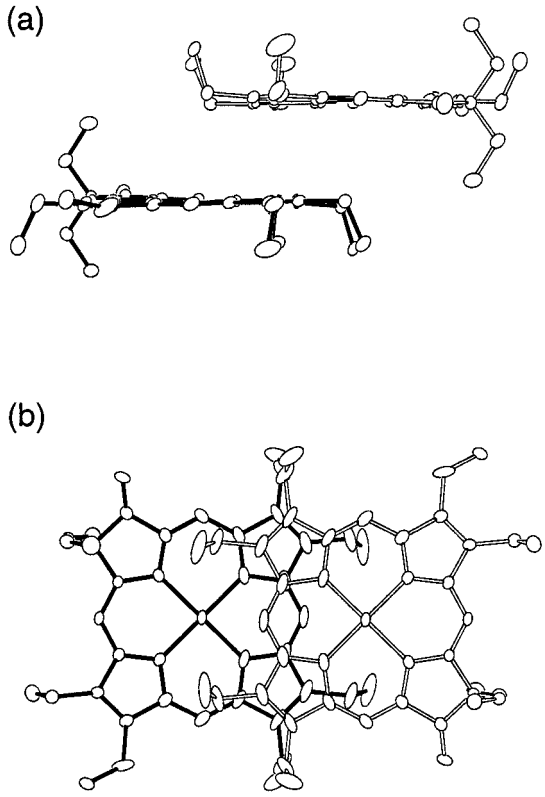

Figure 5. Edge-on view (a) and top-down view (b) of the closest inversion related dimeric unit of [Cu(oxoOEC$^{\bullet}$)][$SbCl_6$].

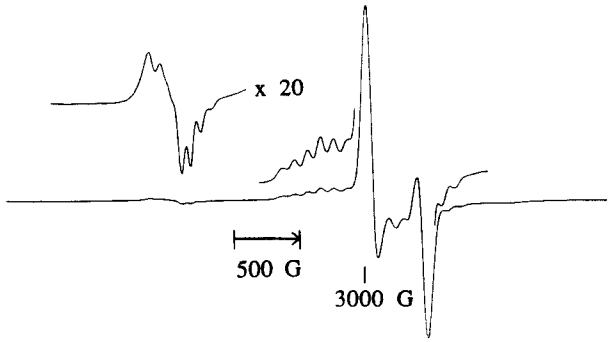

Figure 6. EPR spectrum of [Cu(oxoOEC$^{\bullet}$)][$SbCl_6$] at 77 K in CH_2Cl_2.

that the keto group could be conjugated with the π system of the macrocycle. The structural details for [Cu(oxoOEC)] and [Cu(oxoOEC$^{\bullet}$)][$SbCl_6$] are displayed in Table 3 where they are also compared to other planar Cu(II) porphyrin complexes ([Cu(OEP)] and [Cu(*n*-PrP)]), [Cu(dioxoOEiBC)], and a copper chlorin complex.

Various conformations have been found in metallo-β-oxoporphyrin systems containing more than one reduced ring (dioxoOEiBC and trioxoOEHP).[13] For example, [Fe(Cl)(dioxoOEiBC)][48] and [Cu(dioxoOEiBC)][47] with two adjacent reduced rings have conformations that are domed and planar, respectively, while [Ni(trioxoOEHP)][46] with three reduced rings is ruffled. The S_4-saddled conformation found in [Cu(oxoOEC$^{\bullet}$)][$SbCl_6$] is similar to that of the general position molecule of [Cu(oxoOEC)]. It has been noted in some severely saddled π-cation radical systems that the magnitude of the saddle distortion increases upon oxidation.[22,23] For example, neutral [Cu(OETPP)][22] adopts a saddled conformation in which the β carbons are displaced up and down by 1.1−1.2 Å from the mean 24-atom plane. After oxidation, the saddling of the π-cation radical, [Cu(OETPP$^{\bullet}$)]$^{+}$,[22,23] increases with the β-carbon displacements averaging 1.36 Å. In contrast to these observations, the saddle distortions decrease after oxidation of [Cu(oxoOEC)] to [Cu(oxoOEC$^{\bullet}$)][$SbCl_6$]. The general position molecule of neutral [Cu(oxoOEC)] has a saddled conformation with the

Table 3. Comparison of Bond Parameters among Copper(II) Porphyrins, Copper(II) β-Oxoporphyrins, and Copper(II) Chlorins

compound	M−N	M−N(red)	$C_\beta-C_\beta$	$C_\beta-C_\beta$(red)	$C_\alpha-N-C_\alpha$	$C_\alpha-N-C_\alpha$(red)	ref
[Cu(oxoOEC)]-gen	1.993(10)	2.057(5)	1.351(9)	1.504(9)	105.1(4)	109.5(5)	this work
[Cu(oxoOEC)]-spe	1.985(6)	2.039(7)	1.362(14)	1.493(16)	104.8(6)	109.6(7)	this work
[Cu(oxoOEC•)][$SbCl_6$]	1.987(5)	2.022(3)	1.354(5)	1.513(4)	104.9(3)	108.5(2)	this work
[Cu(OEP)]	1.998(3)		1.347(7)		105.5(3)		68
[Cu(*n*-PrP)][13]	2.000(8)		1.345(8)		106.3(6)		69
[Cu(dioxoOEiBC)]	1.999(10)	2.044(13)	1.362(8)	1.515(9)	105.4(4)	109(1)	47
[Cu(rhodochlorin)],[13] molecule 1	1.994(10)	2.021(8)	1.356(26)	1.586(17)	105.9(10)	106.8(8)	49
[Cu(rhodochlorin)], molecule 2	2.005(10)	2.026(8)	1.373(18)	1.520(19)	105.1(10)	108.4(8)	49
[Cu(rhodochlorin)], molecule 3	2.004(8)	2.028(7)	1.373(15)	1.514(16)	105.1(10)	108.4(8)	49
[Cu(rhodochlorin)], molecule 4	1.994(10)	2.004(10)	1.345(17)	1.520(14)	106(1)	107.1(9)	49

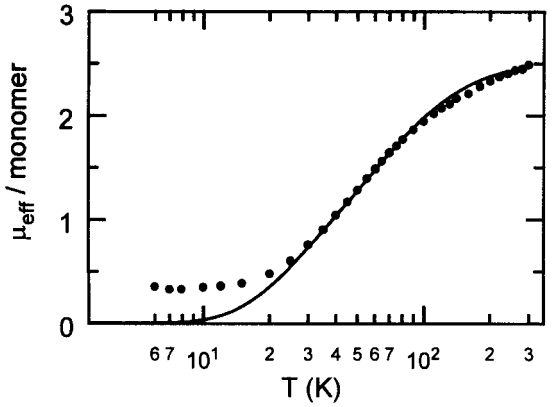

Figure 7. Comparison of observed and calculated values of μ_{eff}/monomer vs T for [Cu(oxoOEC•)][$SbCl_6$]. The solid line is a model calculation assuming spin coupling with $2J_{Cu-Cu} = -70$ cm^{-1}, $2J_{r-r} = -139$ cm^{-1}, and $2J_{Cu-r} = 139$ cm^{-1}.

β-carbon displacements ranging from 0.10 to 0.17 Å and an absolute average of 0.13(2) Å. After oxidation to the π-cation radical, [Cu(oxoOEC•)][$SbCl_6$], the saddled distortion has β-carbon displacements in the range 0.05−0.11 Å, and an absolute average of 0.08(3) Å.

A striking feature of the structure of [Cu(oxoOEC)]-gen and [Cu(oxoOEC•)][$SbCl_6$] is that all ethyl groups, except the *gem*-diethyl group, are on one side of the molecule (see Figures 4a and Figure 5a). In related systems, this type of structural feature is generally indicative[70] of a pairwise inter-ring $\pi-\pi$ interaction. Although complete ring−ring overlap is prevented by the presence of the *gem*-diethyl group, there is clearly an inter-ring interaction between oxochlorin rings in [Cu(oxoOEC)]-gen. Figure 4c shows a top-down view of an inversion-related pair of rings; for this pair the two copper centers are separated by 6.42 Å with a mean plane separation of 3.27 Å and a lateral shift of 5.52 Å. The special position molecules have a very minimal overlap of the two rings as is shown in Figure 4b. The two closest copper centers are separated by 8.51 Å and a lateral shift is 7.75 Å, even though the two rings have a mean plane separation of 3.52 Å.

The inter-ring interactions between the closest pair in [Cu(oxoOEC•)][$SbCl_6$] are shown in Figure 5a. The values describing the interactions are surprisingly similar to those of the neutral precursor, a somewhat surprising feature as noted below. As shown in Table 4, the Cu···Cu distance, the lateral shift, and the mean plane separation are very similar to those of [Cu(oxoOEC)]-gen. However, there are large differences in the exact $\pi-\pi$ overlap (see top-down views, Figures 4c and 5b). Specifically, general position [Cu(oxoOEC)] has overlap at the $C_\alpha-C_{meso}$ and $C_\alpha-N$ positions, while [Cu(oxoOEC•)][$SbCl_6$] has overlaps at $C_\alpha-C_\alpha$ and $C_\beta-C_\beta$. The top-down view of the [Cu(oxoOEC•)][$SbCl_6$] "dimer" (Figure 5b) shows the preferential orientation of the two porphyrin rings that maximize atom−atom contact with a limited *inter*molecular overlap. The two rings are related by an inversion center and the two unique inter-ring contacts are $C_{a6}\cdots C_{a7'} = 3.351$ Å and $C_{b5}\cdots C_{b8'} = 3.498$ Å.

Table 4. Comparison of Geometry among Dimers of [Cu(oxoOEC)] and [Cu(oxoOEC•)][$SbCl_6$]

compound	M···M	Ct···Ct[a]	MPS[b]	LS[c]
[Cu(oxoOEC)]-gen	6.42	6.42	3.27	5.52
[Cu(oxoOEC)]-spe	8.51	8.51	3.52	7.75
[Cu(oxoOEC•)][$SbCl_6$]	6.45	6.42	3.41	5.43

[a] Ct is the center of a 24-atom porphyrin ring. [b] The average mean plane separation for the two 24-atom cores of the dimer. [c] Lateral shift between the two 24-atom cores of the dimer.

The porphyrin−porphyrin ring overlap in this Cu(oxoOEC) π-cation radical system is distinctly different from that of the four- and five-coordinate metallo octaethylporphyrinate (OEP) π-cation radical dimers.[14−16] The OEP π-cation radicals typically form tight cofacial dimers with small lateral shifts. Although the complete overlap of the two rings in [Cu(oxoOEC•)][$SbCl_6$] is prevented by the *gem*-diethyl group, a larger degree of ring−ring overlap than observed would be allowed. Interestingly, the intermolecular geometry of [Cu(oxoOEC•)][$SbCl_6$] resembles that of the six-coordinate vanadyl octaethylporphyrinate π-cation radical, [$VO(OH_2)$(OEP•)]$SbCl_6$.[21] The vanadyl structure also shows a sawtooth edge-over-edge interaction which has minimal $\pi-\pi$ overlap with a V···V distance of 7.46 Å and a mean plane separation of 3.30 Å. Finally, a frequently observed structural pattern in π-cation radical systems is an alternating "long" and "short" bond distance pattern in the inner 16-membered ring.[14−16,22,75] There is no evidence for this pattern in the [Cu(oxoOEC•)][$SbCl_6$] system.

The temperature-dependent magnetic properties of the [Cu(oxoOEC)] and [Cu(oxoOEC•)][$SbCl_6$] derivatives have been measured between 6 and 300 K. As described in the Results, the magnetic susceptibility of [Cu(oxoOEC)] is relatively simple and will not be considered further. The magnetic properties of [Cu(oxoOEC•)][$SbCl_6$] are more interesting.

Detailed studies of magnetic interactions between paramagnetic metal centers and porphyrin π-cation radicals are relatively limited with copper systems the most studied. It has been previously shown that [Cu(TPP•)][$SbCl_6$] is diamagnetic up to temperatures above ambient, consistent with strong antiferromagnetic coupling between the unpaired spin of the copper(II) and the radical.[10] [Cu(TMP•)][$SbCl_6$] is a strongly ferromagnetically coupled system with $S = 1$;[20] the difference between the two derivatives was explained in terms of differences in porphyrin core conformation.[10,11,20] Antiferromagnetic interactions result when the core is nonplanar and ferromagnetic interactions result when the core is planar. The sterically crowded copper(II) π-cation radical, [Cu(OETPP•)]ClO_4, is

(75) Brancato-Buentello, K. E.; Scheidt, W. R. *Angew. Chem.* **1997**, *36*, 1456.

observed to be diamagnetic, again due to strong antiferromagnetic intramolecular coupling between the copper ion and the π-cation radical.[22] The porphyrin ring is both saddled and ruffled, and has well-separated copper ions (Cu−Cu = 8.35 Å) due to the large substituents at the molecular periphery. On the other hand, Fujii[24] reported that [Cu(TMTMP•)][$SbCl_6$][13] displays magnetic susceptibilities that can be fit with modest intramolecular copper−radical antiferromagnetic coupling ($2J_{Cu-r} = -120$ cm^{-1}) and no intermolecular coupling contribution. It is presumed that this is a monomeric copper(II) porphyrin π-cation radical; however, no structural information is available that defines the inter- or intramolecular geometry.

The temperature-dependent magnetic susceptibility data and the EPR spectrum for [Cu(oxoOEC•)][$SbCl_6$] clearly show that this paramagnetic system is more complex than these. An attempted simple monomeric fit (intramolecular copper−radical coupling only) to the temperature-dependent magnetic susceptibility data for [Cu(oxoOEC•)][$SbCl_6$] yields large deviations from the data across the entire temperature range. In addition, the frozen solution EPR spectrum indicates a Cu···Cu interaction; the solution near-IR bands suggest that the system is comprised of dimeric units. Although the solid-state EPR spectrum is poorly resolved, it appears similar to that observed in frozen solution. The possible magnetic exchange interactions involved in the laterally shifted dimeric [Cu(oxoOEC•)][$SbCl_6$] complex includes three interaction types: copper−copper, with coupling constant $2J_{Cu-Cu}$; radical−radical, with coupling constant $2J_{r-r}$; and copper−radical, with coupling constant $2J_{Cu-r}$. The model derived using these interactions must be consistent with both the magnetic susceptibility data and the EPR spectrum.

The EPR spectrum of [Cu(oxoOEC•)][$SbCl_6$] in frozen dichloromethane at 77 K (Figure 6) shows the half-field ($\Delta m_s = \pm 2$) signal characteristic of a dimeric copper(II) triplet state. The EPR spectrum closely resembles the spectra of [Cu(OEP•)]$^+$ and [Cu(OEC•)]$^+$ π-cation radicals at 77 K.[25,26] The splitting of the parallel signal into seven lines can be attributed to the hyperfine structure from two copper nuclei each with $I = {}^3/_2$. Thus the two unpaired electrons of copper give rise to a triplet-state EPR spectrum for [Cu(oxoOEC•)][$SbCl_6$].

The temperature dependence of the effective magnetic moments for [Cu(oxoOEC•)][$SbCl_6$] (Figure 7) can best be fit with a four-spin model. This model includes three terms in the total Hamiltonian: intermolecular interactions between copper centers, $2J_{Cu-Cu}$, intermolecular coupling of the two radical spins, $2J_{r-r}$, and intramolecular magnetic coupling $2J_{Cu-r}$ between the copper spin and the π-cation radical spin. The Hamiltonian of such a system is

$$H = \mu_B \vec{H}\cdot(\tilde{g}\cdot(\vec{S} + \vec{S}') + 2(\vec{s} + \vec{s}')) - 2J_{Cu-Cu}(\vec{S}\cdot\vec{S}') - 2J_{Cu-r}(\vec{S}\cdot\vec{s} + \vec{S}'\cdot\vec{s}') - 2J_{r-r}(\vec{s}\cdot\vec{s}')$$

where S and S' are the Cu spins, s and s' are the radical spins, and the Cu g-tensor is taken to be (2, 2, 2.3).

The intermolecular copper−copper and radical−radical interactions are antiferromagnetic ($2J_{Cu-Cu} = -70$ cm^{-1} and $2J_{r-r} = -139$ cm^{-1}), while the intramolecular copper−radical interaction is ferromagnetic ($2J_{Cu-r} = 139$ cm^{-1}). Modest deviations of the model fit from the experimental data occur at temperatures below 20 K. A better fit to the low-temperature region can be obtained by using a model which includes a completely unrealistic dipolar coupling constant ($J_{dip} \geq -70$ cm^{-1}); however, such a large dipolar coupling constant is not consistent with the calculated transition probabilities for the half-field transition in the EPR spectrum. In general, the interaction between two unpaired electrons will have an isotropic exchange contribution which causes an energy separation between the singlet and triplet $M_s = 0$ energy levels and anisotropic dipolar interaction which shifts the energy of the triplet $M_s = \pm 1$ levels relative to the triplet $M_s = 0$ level.[76,77] Calculations of the powder-average EPR transition probability for various values of the Cu−r dipolar coupling constant of [Cu(oxoOEC•)][$SbCl_6$] result in an observed half-field transition when the dipolar coupling constants are on the order of 0.1 cm^{-1}. This is in agreement with early results which estimate the dipolar coupling strength to be on the order of 0.1−0.3 cm^{-1}.[78] Furthermore, a resolved half-field transition in the EPR spectrum requires the dipolar coupling to be less than the microwave quantum, or 0.3 cm^{-1} at X-band. Thus, the estimated dipolar coupling constant ($J_{dip} = -0.1$ cm^{-1}) explains the observed half-field transition in the EPR spectrum, but has negligible effects on the low-temperature fit to the magnetic susceptibility data. We note that the EPR-active triplet state which is split by the dipolar coupling is an excited state at 64 cm^{-1} above a singlet ground state.

The coupling parameters obtained from the magnetic susceptibility fit for [Cu(oxoOEC•)][$SbCl_6$] parallel those found in the six-coordinate vanadyl octaethylporphyrinate π-cation radical system, [$VO(OH_2)$(OEP•)]$SbCl_6$.[21] In the vanadyl system, the unpaired electron on the metal center is ferromagnetically coupled to the radical ($2J_{V-r} = 63$ cm^{-1}), and the two radical spins are coupled antiferromagnetically ($2J_{r-r} = -139$ cm^{-1}). It is important to note that in both the vanadyl radical cation system and the copper radical cation described here relatively strong antiferromagnetic coupling between the two radical spins is achieved despite the limited ring−ring overlap, i.e., relatively large lateral shifts.

Summary. We have reported the characterization of the first metallooxooctaethylchlorin π-cation radical, [Cu(oxoOEC•)][$SbCl_6$]. The formation of tight cofacial dimeric units, which are characteristic of metallooctaethylporphyrin π-cation radicals, is inhibited by the modification at the periphery of the porphyrin ring. Nonetheless, there is a strong antiferromagnetic interaction between radical spins in a dimeric unit with large lateral shifts. Further, we have been able to obtain reasonable estimates of the various inter- and intramolecular coupling components by the complementary use of X-ray crystallography, temperature-dependent magnetic susceptibility measurements, EPR, and UV/vis/near-IR techniques.

Acknowledgment. We thank the National Institutes of Health for support of this research under Grant GM-38401 (W.R.S.) and for the purchase of X-ray instrumentation under Grant RR-06709. We also thank the National Science Foundation for the purchase of the SQUID equipment under Grant DMR-9703732.

Supporting Information Available: Figure S1 showing the temperature-dependent magnetic susceptibility plot (6−300 K) for [Cu(oxoOEC)]; Tables S1−S12 giving complete crystallographic details, complete listings of bond distances and angles, anisotropic temperature factors, and fixed hydrogen atom positions for both complexes (23 pages). An X-ray crystallographic file, in CIF format, for [Cu(oxoOEC•)][$SbCl_6$] only. This material is available free of charge via the Internet at http://pubs.acs.org.

IC9903026

(76) Eaton, S. S.; More, K. M.; Sawant, B. M.; Eaton, G. R. *J. Am. Chem. Soc.* **1983**, *105*, 6560.
(77) Eaton, S. S.; Eaton, G. R. *J. Am. Chem. Soc.* **1982**, *104*, 5002.
(78) Schulz, C. E.; Rutter, R.; Sage, J. T.; Debrunner, P. G.; Hager, L. P. *Biochemistry* **1984**, *23*, 4743.